Fuel cell and Li-ion battery direct hybridization system for aircraft applications

Akira Nishizawa [a,*], Josef Kallo [b], Olivier Garrot [b], Jörg Weiss-Ungethüm [b]

[a] Japan Aerospace Exploration Agency (JAXA), 7-44-1 Jindaiji Higashimachi, Chofu, Tokyo 182-8522, Japan
[b] Deutsches Zentrum für Luft-und Raumfahrt (DLR), Institut für Technische Thermodynamik, Pfaffenwaldring 38-40, D-70569 Stuttgart, Germany

HIGHLIGHTS

► We verified a concept of FC-Battery direct hybrid system without DC/DC converters.
► The dynamic behavior of the hybrid system was clarified through the experiments.
► A design method of direct hybrid system was suggested for aircraft applications.

ABSTRACT

The concept of a passive hybrid system consisting of fuel cell stacks, Li-ion battery packs, and two diodes was tested. The diodes take the place of the DC/DC converter that is usually used to align fuel cell and battery voltages, thereby directly connecting the fuel cell and the battery. Prototype equipment was built for collecting characteristic data on the static and dynamic behavior of the hybrid system. The measurement results indicate that increasing the operation efficiency and simplifying the system were possible by applying the direct hybridization concept. The dynamic behavior results showed an interesting combination of output signals from the fuel cell stack and the battery pack. The quick response of the battery output completely compensated for the delay in fuel cell output response, indicating that the direct hybrid system is also applicable to high-frequency electric loads such as brushless DC motors. The ability to recharge without a DC/DC converter was also successfully validated for the direct hybrid system. From the measurement results, the design method, and the system sizing, this passive hybrid system appears promising for application in the Antares DLR-H2 electric aircraft test bed.
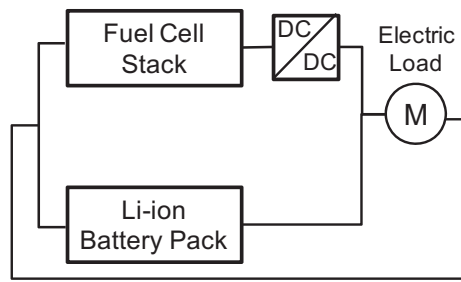
© 2012 Elsevier B.V. All rights reserved.
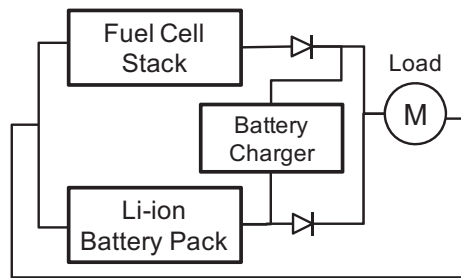
1. Introduction

Fuel cell systems are a key new technology for improving aircraft efficiency. Global players in commercial aircraft industry like Boeing and Airbus have begun considerable research into fuel cell systems, focusing on the use of fuel cells to eliminate several conventional systems with the goal of creating more-electric aircraft and multiple new functions such as nose wheel drive and onboard water generation [1,2]. Fuel cell systems can also provide, without assistance, all the main propulsion power for small airplanes in a similar way as with fuel cell electric cars. Small, fuel cell-powered airplanes have succeeded in flying in recent years [3–5]. These trends indicate that fuel cell systems in aircraft applications may change the face of aviation. The present paper aims to investigate the characteristic features of a direct hybrid system used in an aircraft application.

It is well known that coupling a fuel cell system with electric energy storage devices can lead to better performance than operating with just a fuel cell system as a power source [6]. Thus rechargeable batteries or supercapacitors are connected in parallel to boost the fuel cell power during increased system load demands. These hybrid systems might be separated into active or passive systems [7]. An active hybrid system often uses DC/DC converters to actively control the power sharing between the fuel cell and the storage device because the voltage of each power source is usually inconsistent. The passive hybrid system directly connects the fuel cell and storage device to the DC bus without the use of power converters. A passive hybrid configuration with direct bus connection has the advantages of low power loss, low cost, and simple architecture due to the lack of DC/DC converters; however a highly constrained special operating procedure is necessary in order to avoid discrepancies in the current–voltage behavior of the fuel cell and the battery. Bernard et al. [8] showed that their original passive hybrid technique was feasible for electric power trains. In their architecture the output power of a polymer electrolyte fuel cell (PEFC) can be arbitrarily changed by adjusting the H_2 and O_2

* Corresponding author. Tel.: +81 50 3362 4458; fax: +81 422 40 3245.
  E-mail address: nishizawa.akira@jaxa.jp (A. Nishizawa).

a Conventional hybrid system.

b Direct hybrid system.

Fig. 1. Hybrid system configurations composed of fuel cells and batteries.

operating pressures. Their system allows the PEFC stack current to be decreased at a constant voltage as the pressure is decreased, which makes it possible to use the passive hybrid system for power train applications with higher efficiency, but the pure oxygen tank is generally not suitable for aircraft applications due to its weight.

In the present paper, we propose a passive hybrid system optimized for aircraft applications. As opposed to one of the most common hybrid systems that uses one DC/DC converter (Fig. 1(a)), our concept of direct hybridization is illustrated in Fig. 1(b). The direct hybrid system is composed of a H_2/Air PEFC stack and a battery pack. The most important aspect of the system is that the DC/DC converter is replaced by two diodes, each connected in serial with one of the power sources. This layout enables the fuel cell to be directly connected to the battery pack in parallel. A basic two

diode configuration was also proposed by Zhuo et al. [9], who developed a new algorithm to minimize charging loss. Here, we focus on the static and dynamic behavior of the direct hybrid system in aircraft applications. The diode which is connected in serial with the battery pack avoids unintentionally recharging of the battery. The diode which is connected in serial with the fuel cell stack avoids reversal current through the fuel cell stack in case of overvoltage at the pins of the load. However, in case of proper system design this diode is only necessary if the load is able to deliver power e.g. by recuperation. This paper describes the behavior of the direct hybrid system in detail and discusses a system design method for aircraft applications.

2. Experimental setup

Prototype test equipment was built in order to obtain characteristic data on the static and dynamic behavior of the hybrid system; the system setup is shown in Fig. 2. A 42-cell PEFC fuel cell stack was used as the main power source, and two Li–FePO$_4$ battery packs were used for hybridization. Each battery block consisted of eight individual cells, four pairs of parallel cells which were serial connected to the pack. The fuel cell stack and battery pack outputs were connected to a controllable electric load each through a diode. A MOS-FET was installed in parallel to the diode of the battery line to recharge the circuit. Two relays were installed in the system for the ability to open the circuit in case of emergency only, but were not essential to the system.

Pure hydrogen and ambient air is automatically supplied to the stack by a programmable, PC-based management system. The static pressure of the hydrogen at the anode inlet is maintained within a range of 25 kPa–30 kPa by a manual pressure regulator. The anode outlet is kept closed by a solenoid valve, except during periodic purges. In this system the anode gas is operated without any recirculation.

A compressor passes ambient air through a passive humidifier into the cathode. The temperature of the cathode exhaust air is kept around 50 °C by a cooling fan with heat sinks, and the mass flow rate of the supply air is optimally controlled by feedback from the monitored cathode exhaust air temperature.

The fuel cell system requires periodic purges to remove the water and nitrogen from the anode. The time intervals between purges depend on the time integration of fuel cell current with the
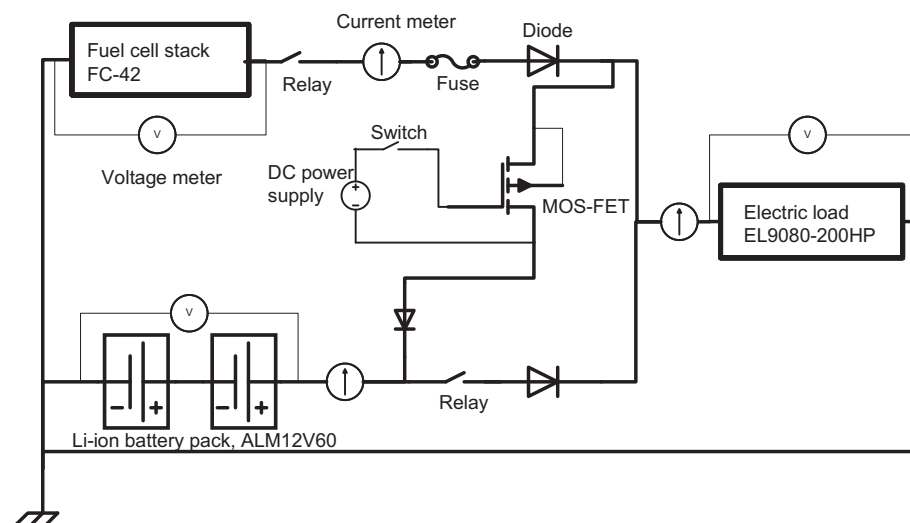
Fig. 2. Electric circuit of the direct hybrid system.

Table 1
Specification for each component.

| Component	Product name (industry)	Specifications and remarks
Fuel cell	FC-42 (schunk)	Nominal current: 15 A Nominal power: 360 W Max current: 30 A It was operated by air cooling with heat sink.
Battery	ALM12V60	Nominal voltage: 12 V Nominal capacity: 4.32Ah@1C discharge) Max. discharge current: 80 A Two packs were connected in series
Electric load	EL9080-200HP (elektro-Automatik)	Current range: 0–200 A It was externally controlled by the control system
Diode	40CPQ060 (IOR)	Max. average forward current: 40 A Max. working peak reverse voltage: 60 V
MOS-FET	PSMN005-75P (PHILIPS)	Drain-source voltage: 75 V Drain-current: 75 A On-state resistance: 5 mΩ
Current transducer	LTS 25-NP (LEM)	Measuring range: 0...±80 A
Control system	TopMessage (Delphin Technology)	Max. sampling rate: 50 Hz/ch. One master module and seven slave modules were managed by a PC.

threshold value of 80 As in the hybrid system. For example, the time intervals are 5 s at 16 A and 10 s at 8 A. No significant effect of voltage decline between the purges is observed in the whole measured data.

The voltage and current of each component are measured by sensors; Table 1 shows detailed equipment specifications for each component.

Fig. 3 shows the characteristic curves of voltage and power versus current for fuel cell stack operation in the case of no battery packs. The electric load current was gradually increased at a rate of 0.1 A s^{-1}; the result produces typical curves for the fuel cell stack and shows that the main power is available up to 400 W.

3. Static behavior of the hybrid system

Fig. 4 shows the quasi-static behavior of the hybrid system during a gradual increase of the electric load current. When the load current starts to rise, only the fuel cell can feed current to the electric load, and the fuel cell voltage rapidly decreases. It is not until the voltage of the fuel cell reaches the same voltage as the
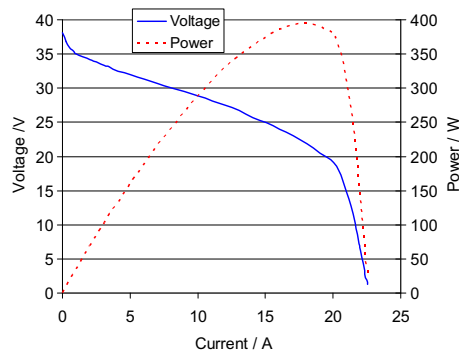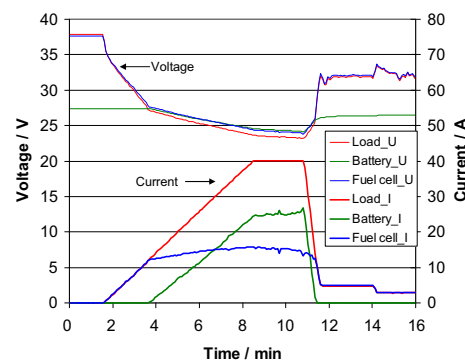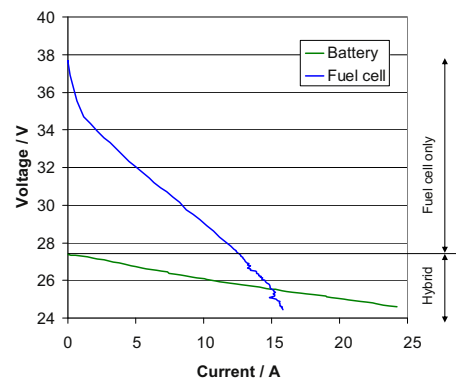
Fig. 4. Time traces of voltage and current for the hybrid system. (The electric load current was gradually increased at the rate of 0.1 A s^{-1}.)
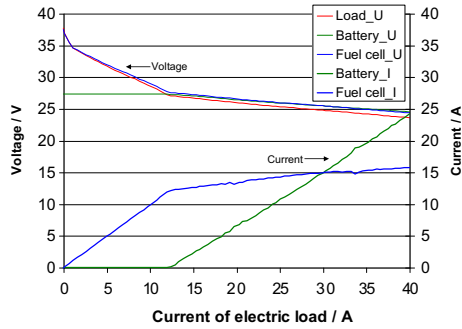
battery that the battery starts to feed its current into the load together with the fuel cell. After the fuel cell and battery voltages met, each voltage decreases in maintaining the value at the exact same level, and the fuel cell current becomes saturated due to a lack of cooling, causing the battery current to exceed the fuel cell current.

Characteristic curves for the fuel cell and battery are obtained, as shown in Fig. 5, by re-plotting Fig. 4. It is a necessary requirement of the direct hybrid system that the voltage operation ranges of both individual components overlap. As the open circuit voltage (OCV) of the battery is about 27.5 V; if the fuel cell voltage is higher than the OCV of the battery, only the fuel cell can feed current into the system load. As voltage of fuel cell and battery equals due to raising system load, the battery come into operation. In hybrid mode, as the slopes of the fuel cell and the battery polarization curves are different, the battery current increases faster with raising load current than the fuel cell current.
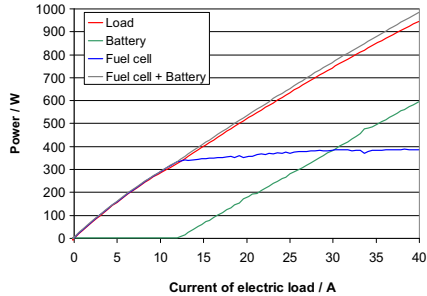
Fig. 6(a) and (b) present variations in electric load current parameters, clearly showing, that the additional current and power can be provided by the battery in accordance with the load current requirements. Passive power sharing reliably occurs between the fuel cell and the battery. Fig. 6(b) shows that the summation of the output powers from the fuel cell and the battery does not agree with the power consumption at load; this discrepancy is plotted in Fig. 7. The gross power is defined as the summation of the output powers from the fuel cell and battery, and the power loss is defined as the difference between the gross power and the power consumption at load. The power loss increases with the increase of the gross power due to losses at the diodes, cupper cables,

Fig. 3. Voltage, current, and power characteristic curves for the fuel cell stack, FC-42. (Data were obtained by increasing the current at 0.1 A s^{-1} while keeping the cathode exhaust gas temperature around 50 °C.)

Fig. 5. Voltage and current characteristic curves for the fuel cell stack and the Li-ion battery pack during hybrid operation. (Data were re-plotted from Fig. 4 during load current rise.)
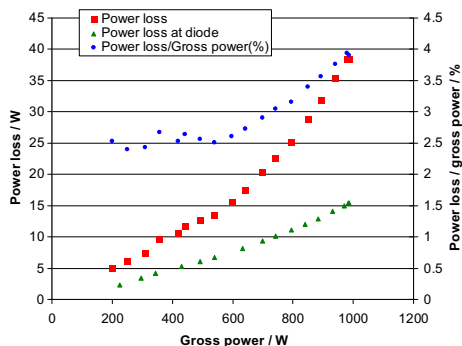
a Voltage and current variations.

b Power variations. (The load power indicates the net power while the summation of fuel cell and battery powers indicates the gross power.)

Fig. 6. Variations of the electric load current parameters during hybrid operation.

Fig. 7. Total power loss and power loss at diodes for the variable gross power.

Fig. 8. Dynamic behavior of the hybrid system. (The electric load current is changed at a rate of 1 A s^{-1} then kept at a constant value for 30 s)

tends to damage the fuel cell. The figure shows that the fuel cell current can follow the load current until the fuel cell voltage meets the battery voltage. The overall system behavior appears to be nearly symmetric for the rising and falling phases of load current. These results indicate that the fuel cell response is sufficient to supply current at the rate of 1 A s^{-1}, and that the battery compensates for the fuel cell only when the fuel cell output approaches saturation.

Fig. 9 shows the cases at a load current rate of 165 A s^{-1}. The maximum and minimum current values and the duration time at constant current are the same as in Fig. 8, but Fig. 9 shows different behavior. The battery current is observed in the case with the maximum value of 12 A, whereas no battery current is observed in Fig. 8. Furthermore the behavior is notably asymmetric for the rising and falling load current phases, except in the 6 A case.

Fig. 10 captures the system behavior details as the load current rises; Fig. 10(a) shows that in the 12 A case, the fuel cell current can rapidly increase as the load current increases, but it quickly decreases due to the finite capacitance of the fuel cell stack. The battery completely compensates for the lack of current provided by the fuel cell. In Fig. 10(a) the time constant in the fuel cell stack can be roughly estimated to be around 2 s. For the 24 A and 36 A cases shown in Fig. 10(b) and (c), respectively, the trends of the fuel cell and battery behavior are similar to those in Fig. 10(a). The fuel cell current rapidly increases as the load current increases, then decreases quickly until finally gradually increasing again. Such dynamic fluctuations in the fuel cell current are completely compensated for by the battery current.

4. Dynamic behavior of the hybrid system

In this section the dynamic behavior of the hybrid system was observed by controlling the electric load at higher current variation rates. Fig. 8 shows the four different fuel cell and battery response cases for the trapezoidal waveforms. The load current is increased and decreased at a rate of 1 A s^{-1}. The maximum current values were maintained at 6 A, 12 A, 24 A, and 36 A during 30 s for each case while the minimum current value was 3 A for all cases. It should be noted that the operation at 0 A as the minimum current was avoided because the operation at OCV with 0 A of fuel cell
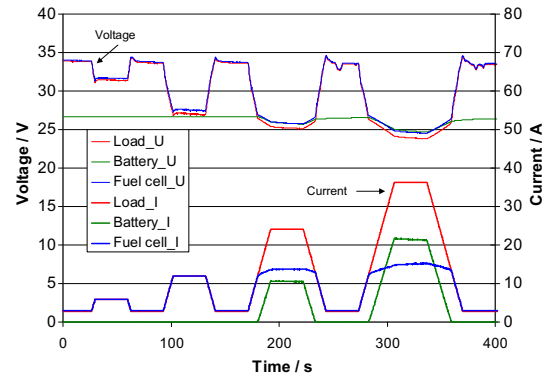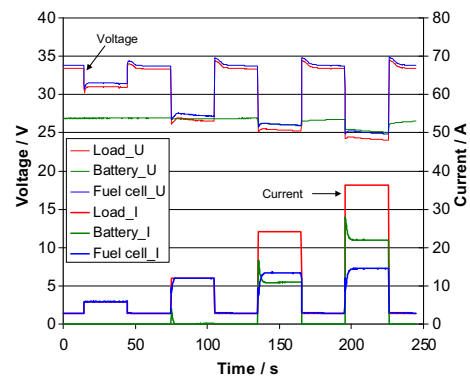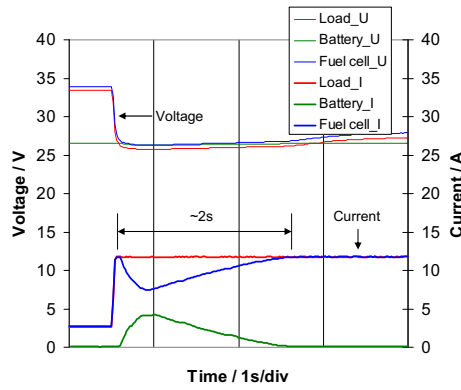
connectors, and relays. At the maximum gross power of 1 kW, the power loss is about 4%, and the power loss contribution from the diodes is less than 2%. This result indicates the direct hybrid system's potential to be highly efficient.

Fig. 9. Dynamic behavior of the hybrid system. (The electric load current is changed at a rate of 165 A s^{-1} then kept at a constant value for 30 s)

a Case with maximum load current of 12 A.
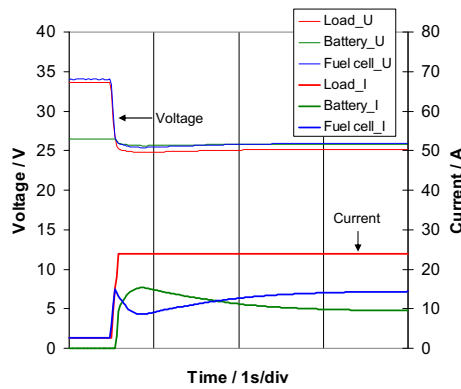
**b** Case with maximum load current of 24 A.
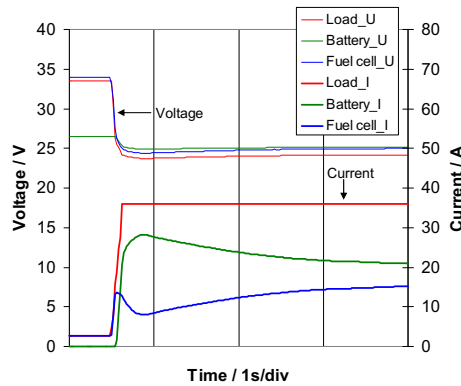
c Case with maximum load current of 36 A.

Fig. 10. Detailed behavior at load current rise captured from Fig. 9.

Fig. 11 demonstrates the cyclic operation at a frequency of 2.5 Hz. The fuel cell current response is variable in each cycle; however, the battery successfully compensates for the variations to keep the exact same wave form of load current in every cycle.
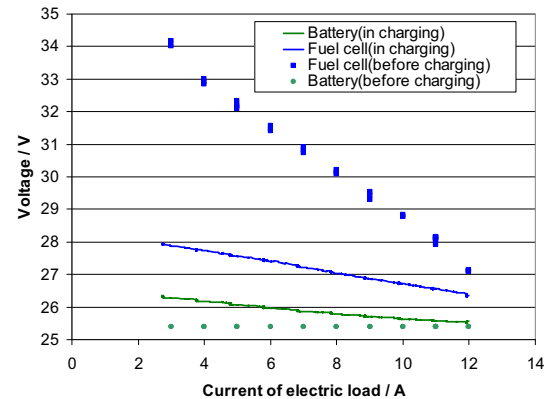
5. Recharging characteristics

Onboard recharging is an essential hybrid system function in aircraft applications. In the present system the recharging was conducted by turning the gate-source voltage at the MOS-FET on
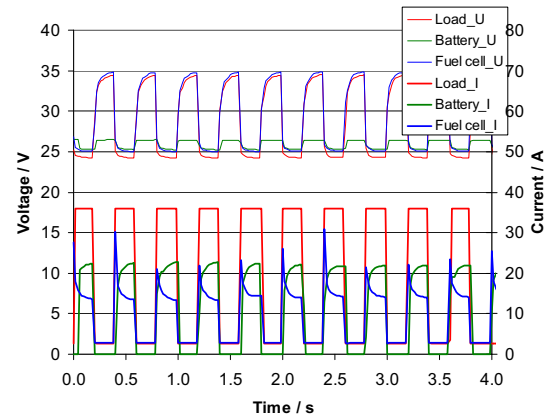

Fig. 11. Demonstrating cyclic operation at a frequency of 2.5 Hz.

and off, as shown in Fig. 2. During the entire testing phase the gate-source voltage was maintained at a constant value of 4.8 V, which is sufficient to lead the current from the drain to the source without any regulation. The MOS-FET was used only as an on-off switch in the system because it can minimize the power loss at the switch during recharging.

Fig. 12 shows the charging characteristics of the hybrid system. The voltage and current of the fuel cell and battery were measured for the variable load currents and the differences were compared

a Variation of voltage.
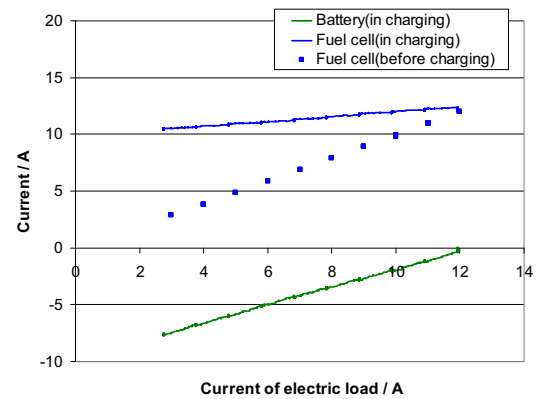
b Variation of current.

Fig. 12. Charging characteristics of the hybrid system at variable electric load currents.
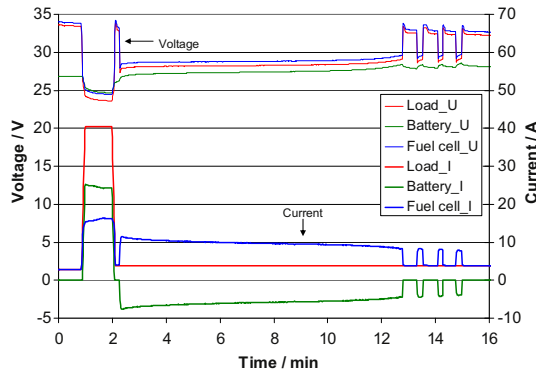
Fig. 13. Demonstrating the total hybrid system behavior, including during the charging phase.

for periods before and during recharging. To avoid the influence of the differences in state of charge, the electric load current was changed stepwise by 1 A for periods of only 5 s. The important feature of this system is, the charging current depends on the load current (Fig. 12(b)).

Fig. 13 shows the overall hybrid system behavior, including the charge phases. After the battery delivers a boost it is recharged by the fuel cell. As the battery voltage gradually increases during the recharge phase, it reaches the maximum acceptable voltage, where feeding current into the battery is stopped by the system controller to avoid excessive battery voltage. As the battery voltage decreases slowly at zero current recharge is started again until the voltage reaches a certain level, where the battery is charged again. The system can repeat this procedure as necessary until the battery is full charged.

It is fairly obvious that the time of continuous operation in hybrid mode completely depends on the battery capacity. The battery capacity should be designed based on the mission. As for aircraft applications the duration time of maximum power output with battery boost during climb phase is generally much shorter than the time of operation with only fuel cell in cruise. This power distribution easily enables the system to recharge the battery using the fuel cell current in the cruise phase, which results in a sustainable operation of the hybrid system.

6. Hybrid system design method

A design method for the direct hybrid system is proposed in this section based on the measurement results described in the
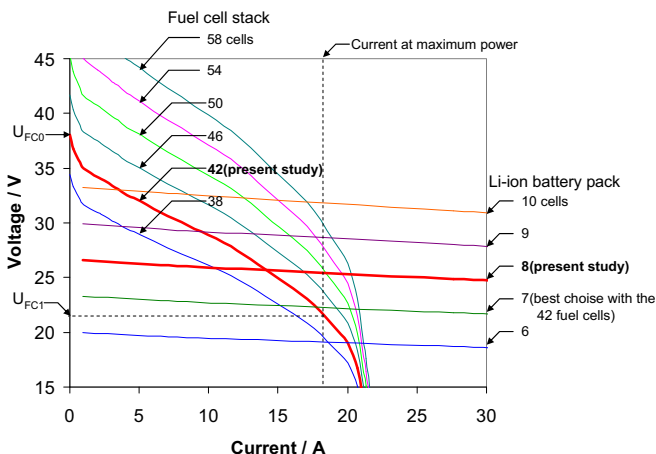
previous sections. For the direct hybrid system, power sharing is one of the most important issues because it should be pre-determined by fuel cell and battery sizing. Fig. 14 shows the combination map of the number of cells for the fuel cell stack and Li-ion battery pack in the hybrid system. The following procedure should be used to select the number of cells.

Step 1: Select the number of cells for the fuel cell stack to satisfy the required power.
Step 2: Define the maximum acceptable voltage, U_{FC0}, for the selected fuel cell stack.
Step 3: Define the voltage at maximum power, U_{FC1}, for the selected fuel cell stack.
Step 4: Select the number of cells for the battery so that the OCV of battery,

U_{BA0}, is in the range of $U_{FC1} < U_{BA0} < U_{FC0}$ and the minimum voltage at maximum current, U_{BA1}, is close to U_{FC1} as $U_{BA1} \approx U_{FC1}$.

For example, if we decide to use the 42-cell fuel cell stack (Fig. 14), we can select from 7 to 10 cells for the battery to create a feasible direct hybrid system. Within this battery cell selection, the 7-cell Li-ion battery is the optimal pairing for the 42-cell fuel cell stack because if U_{BA0} is slightly higher than U_{FC1} we can obtain the approximate maximum power from the fuel cell, as described below in detail. In the design of the hybrid system the battery capacity has no effect on the supply power ratio between the battery and fuel cell. Therefore it is very easy to increase the operation time with battery capacity by connecting additional battery cells in parallel, independently of the main design parameters such as number of cells connected in series for each of battery and fuel cell.

For a final demonstration of the hybrid system design method, fuel cell and battery sizes were evaluated based on the electric fuel cell motor of the Antares DLR-H2 glider [2,4]. The Antares DLR-H2, which was remodeled from the Antares 20E glider electric battery motor, developed by DLR to study fuel cell technology for aircraft applications [10]. It can fly an entire flight phase using only fuel cell power, independent of any hybrid operation or batteries; however, its climbing performance would be expected to improve with the addition of the hybrid system's power boost. In this section the optimum number of battery cells is discussed under the assumption that the direct hybrid system was applied to the Antares DLR-H2.

Fig. 15 shows the characteristic current and voltage curves for the fuel cell stacks and battery packs, assuming their application in the Antares DLR-H2. It has four high-temperature proton exchange membrane stacks in series-parallel connection. The plotted data for
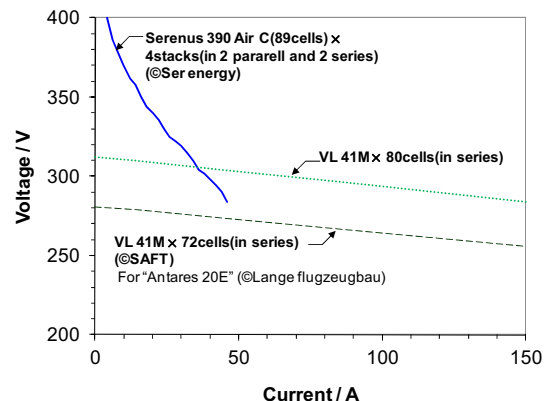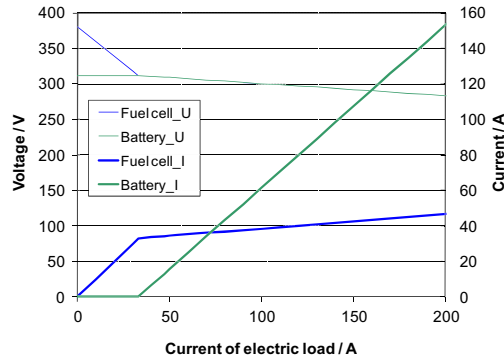

Fig. 14. Combination map of the number of fuel cell stack cells and Li-ion battery packs in the hybrid system.
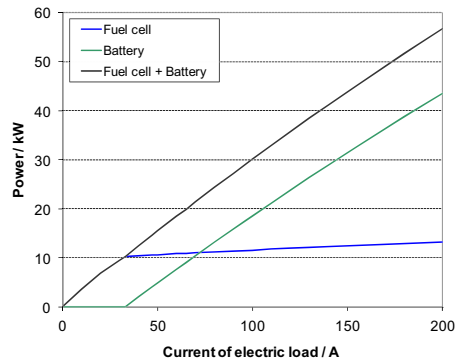

Fig. 15. Characteristic current and voltage curves for the fuel cell stacks and battery packs assuming the application to Antares DLR-H2.

a Voltage and current variations.

b Power variations.

Fig. 16. Predicted static behavior of the direct hybrid system. The system is composed of an 80-cell battery in series and a 4-pack fuel cell stack (2 in series and 2 in parallel).

the stacks were obtained from literature in the industry. The original Antares 20E had a 72-cell battery connected in series; its battery data were also obtained from industry literature. The combination of a 72-cell battery and a fuel cell stack indicates that hybrid operation is not feasible because the open circuit voltage of the 72-cell battery does not satisfy the necessary requirement of $U_{FC0} > U_{BA0} > U_{FC1}$. Therefore the number of cells in the battery has to be increased to satisfy the requirement. When the number of cells is increased to 80, the battery curve overlaps the operating voltages of the fuel cell stack. The static behavior of the hybrid system in question can easily be predicted in the following manner:

$$I_{EL} = I_{FC}, I_{BA} = 0 (\text{when } U_{FC} > U_{BA0})$$

$$U_{FC} = U_{BA}, I_{EL} = I_{FC} + I_{BA} (\text{when } U_{FC} \leq U_{BA0})$$

here, I and U represent the current and the voltage, respectively. The subscripts EL, FC, and BA indicate the electric load, the fuel cell, and the battery, respectively.

Fig. 16 shows the predicted static behavior of the hybrid system. In this prediction we considered the lower limitation of the fuel cell stack voltage, therefore the behavior is only illustrated up to the point that the fuel cell stack voltage reaches the limitation at around 280 V. If we have to avoid such low voltage situations for safety reasons, it is important to consider lower operating voltage limits. Fig. 16(a) indicates that the battery can provide current up to its upper limitation because the minimum voltage at the maximum current, U_{BA1}, is nearly equal to the lower voltage limitation of the fuel cell for this combination of cell numbers. In this case the lower fuel cell voltage limitation is equal to U_{FC1}. It is found that the boosted total power reaches 55 kW while the fuel cell output power can reach only 13 kW (Fig. 16(b)). These prediction results imply that the direct hybridization concept is applicable to a manned electric aircraft propulsion system.

7. Conclusion

A fuel cell and battery direct hybrid system concept without DC/DC converters was proposed. The system concept was validated by measurements using an electric system composed of a low-temperature PEFC stack and Li–FePO$_4$ battery blocks. The measurements showed good system efficiency and good response to dynamic load requests. A direct hybrid system design method was suggested and the system behavior was predicted for the Antares DLR-H2. Onboard battery recharging can also be achieved by a simple circuit configuration without a DC/DC converter. The direct hybrid system has a potential to achieve high efficiency operation with a simple system configuration.

References

[1] Airbus International Press Release, Airbus and German Aerospace Centre (DLR) Perform Research Tests for Fuel Cell Powered Autonomous Taxiing (6 July 2011).http://www.airbus.com/en/presscentre/pressreleases/pressreleases_items/.
[2] K.A. Friedrich, J. Kallo, J. Schirmer, G. Schmitthals, Fuel cell systems for aircraft application, ECS Transactions 25 (1) (2009) 193–202.
[3] Boeing news release, Boeing Successfully Flies Fuel Cell-Powered Airplane (2008).http://www.boeing.com/news/releases/2008/q2/080403a_nr.html.
[4] DLR National Press Release, DLR Motor Glider Antares Takes off in Hamburg-powered by a Fuel Cell (7 July 2009).http://www.dlr.de/en/desktopdefault.aspx/tabid-344/1345_read-18278/.
[5] G. Romeo, F. Borello, G. Correa, ENFICA-FC: Design, Realization and Flight Test of all Electric 2-Seat Aircraft Powered by Fuel Cells, 27th International Congress of the Aeronautical Sciences (ICAS2010), 2010.
[6] B. Davat et al., Fuel cell-based hybrid systems, Advanced Electromechanical Motion Systems & Electric Drives Joint Symposium, 2009, ELECTROMOTION 2009, 8th International Symposium, 2009 1–11.
[7] R. Saïsset, C. Turpin, S. Astier, J.M. Blaquière, Fuel cell/battery passive hybrid powertrain with active power sharing capability, IEEE Vehicle Power and Propulsion Conference 2004.
[8] J. Bernard, M. Hofer, U. Hannesen, A. Toth, A. Tsukada, F.N. Büchi, P. Dietrich, Fuel cell/battery passive hybrid power source for electric powertrains, Journal of Power Sources 196 (2011) 5867–5872.
[9] J. Zhuo, C. Chakrabarti, N. Chang, S. Vrudhula, Extending the lifetime of fuel cell based hybrid systems, DAC '06 Proceedings of the 43rd Annual Design Automation Conference, 2006 562–7.
[10] http://www.lange-aviation.com/htm/english/products/antares_20e/antares_20E.html